

The alcohol productivity of this catalyst at 295°C during the Set 1 experiments appeared to be anomalously low compared to the 285, 300, and 310°C testing results. For example, the total alcohol productivities at these temperatures were 136.2, 138.8, and 135.3 g/kg cat/hr, respectively. Over an earlier tested 10 wt% CsOOCH/MoS<sub>2</sub> catalyst [11,65], the alcohol productivity under approximately the same reaction conditions was ≈240 g/kg cat/hr. Therefore, the present catalyst is significantly less active than the 10/90 wt% CsOOCH/MoS<sub>2</sub> catalyst prepared earlier [11,65]. Although this is a low activity catalyst, the experiments indicate that partial deactivation tended to increase the yield of hydrocarbon at lower reaction temperatures but to lower the productivity of the hydrocarbons at higher reaction temperatures. Further work is need to understand this catalytic behavior.

Testing 10 wt% CsOOCH/MoS<sub>2</sub> Catalyst-Sample 2. A second sample of 10 wt% CsOOCH/MoS<sub>2</sub> catalyst was tested, and the sample was protected against air exposure during its preparation steps. This catalyst was Sample 2, as designated in the Experimental Section, and it was prepared by decomposing undiluted MoS<sub>3</sub> in a N<sub>2</sub> flow, transferring to a vacuum apparatus (Figure 12), and doping with CsOOCH. The catalyst (1.7313 g) was mixed with Pyrex beads and loaded into the reactor under N<sub>2</sub> to form a bed approximately 12 cm in height in the reactor. The catalyst was reductively pretreated with H<sub>2</sub>/N<sub>2</sub> = 2/98 vol% gas flowing at 60 ml/min. The temperature was slowly increased to 400°C, and CO<sub>2</sub> and H<sub>2</sub>O were monitored by gas chromatography, while H<sub>2</sub>S was monitored by lead acetate paper. Hydrogen sulfide was first detected at 191°C and was still present in the exit gas after 1 hr of pretreatment, at which time the temperature was decreased to ambient conditions. No H<sub>2</sub>O nor CO<sub>2</sub> was detected. After cooling, the catalyst was maintained in the H<sub>2</sub>/N<sub>2</sub> mixture overnight prior to catalytic testing.

After setting the  $\text{H}_2/\text{CO} = 1/1$  synthesis gas flow rate to  $\text{GHSV} = 7758 \text{ l/kg cat/hr}$ , the reactor was pressurized to 8.3 MPa and then heated to 245°C. The reaction temperature was then increased sequentially to 256, 265, 275, and 295°C. The exit stream was sampled and analyzed every 33 min using an on-line GC. Liquid products were also collected for GC/MS analyses.

Steady state conversions were maintained for 20-40 hr at each reaction temperature, as shown in Figure 62. The CO conversion at 265°C corresponded to 4.7% conversion to products. As the reaction temperature was progressively increased, the productivities of the alcohols, hydrocarbons, and carbon dioxide increased, as shown in Figures 63 and 64. A high productivity to linear alcohols was observed at 295°C, as indicated in Figure 63. At each temperature, the dominant alcohol formed was methanol, compare Figure 65 with Figure 63.

At all temperatures, the alcohols were the principal products. However, a significant selectivity toward hydrocarbon formation, typical for alkali/ $\text{MoS}_2$  catalysts, was observed, as shown in Figure 66. This is further reflected by the plot shown in Figure 67 of the alcohol/hydrocarbon molar ratio for the products formed at each temperature. The average space time yields of the alcohols and total hydrocarbons are shown in Figures 68 and 69. There was hardly any noticeable trend toward the formation of higher molecular weight alcohols relative to methanol as the reaction temperature was increased, see Figure 70.

This  $\text{CsOOCH}/\text{MoS}_2 = 10/90 \text{ wt\%}$  catalyst was an active catalyst, and this is demonstrated by the data in Table 13. The comparison with a previously tested catalyst [11], included in Table 13, shows that the present catalyst was slightly less active at lower reaction temperatures but slightly more active at higher temperatures. Some apparent deactivation occurred at 295°C, see Figures 62 and 65. Upon returning to a reaction

FIGURE 62. CO CONVERSION RATE VS TIME

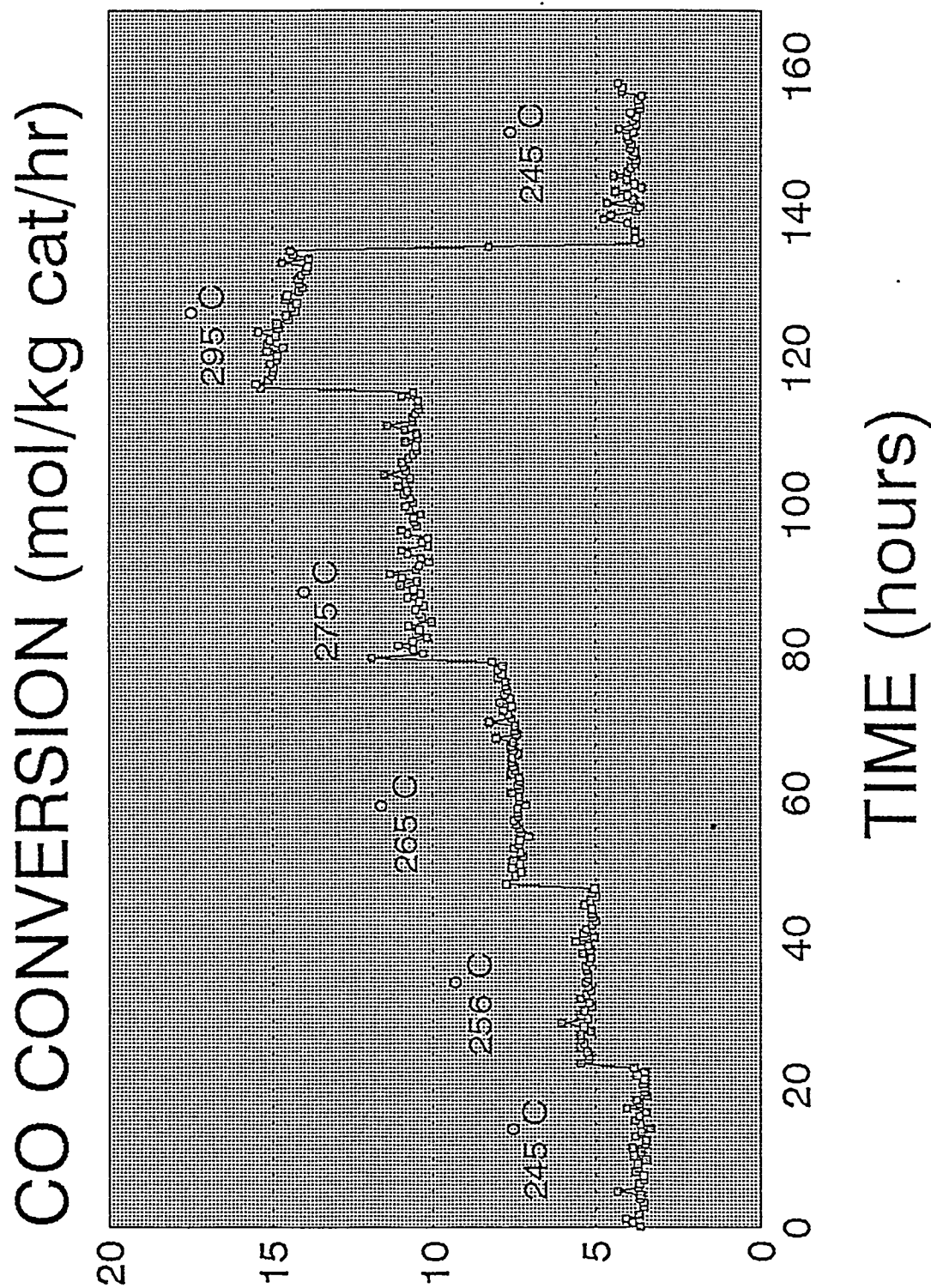


FIGURE 63. TOTAL ALCOHOL AND HYDROCARBON SPACE TIME YIELDS VS TIME

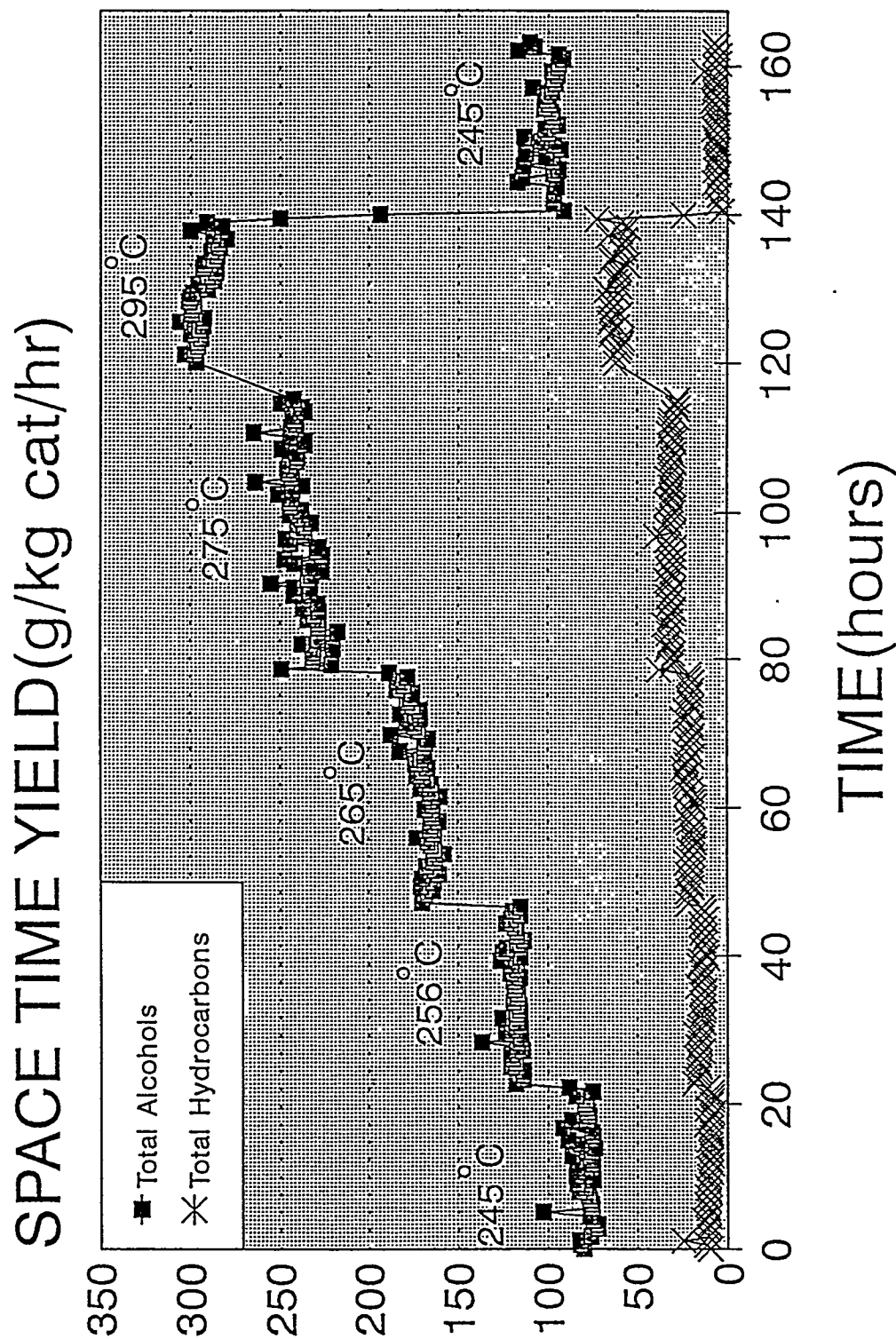


FIGURE 64. CARBON DIOXIDE SPACE  
TIME YIELDS VS TIME

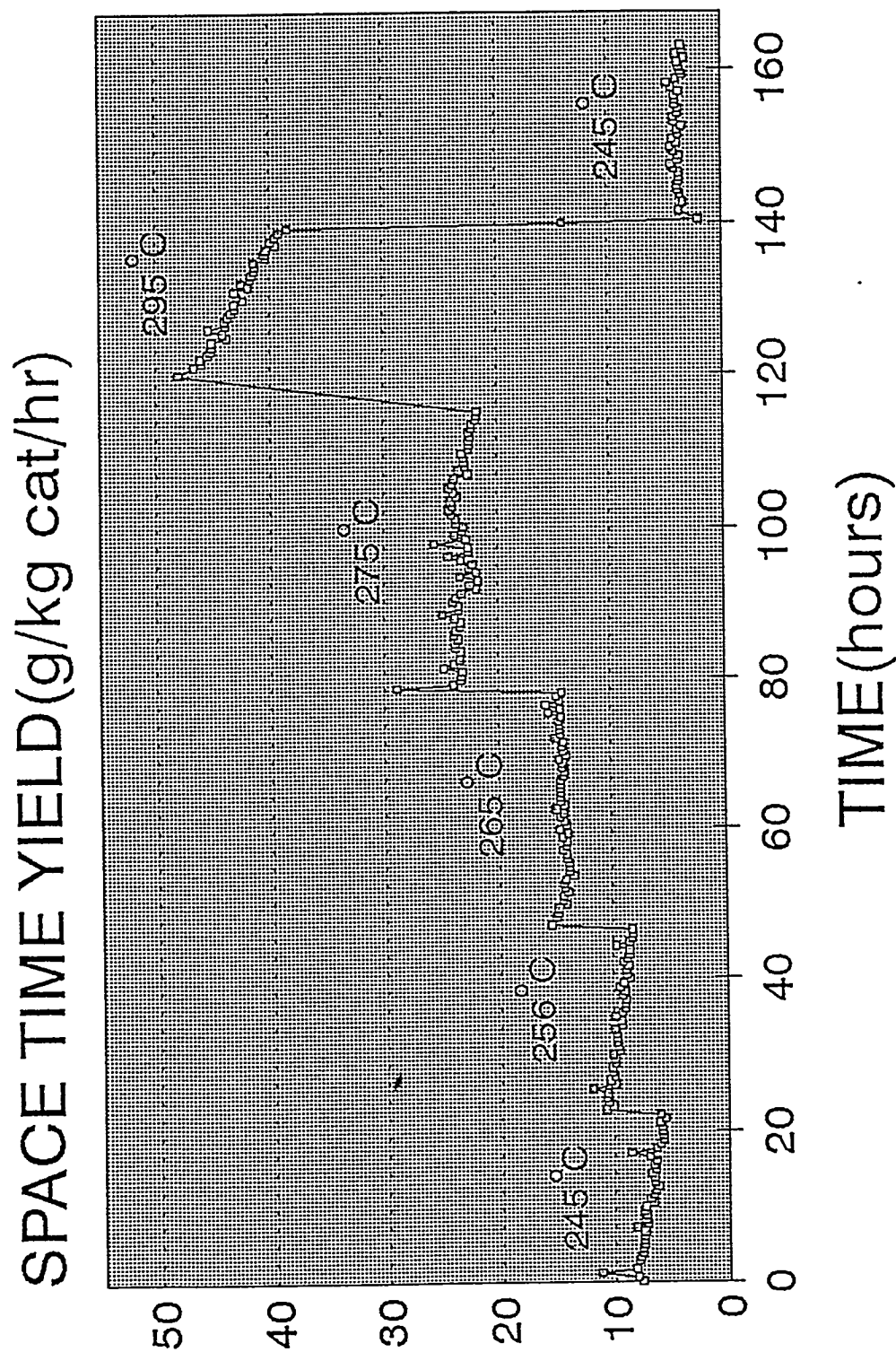


FIGURE 65. METHANOL SPACE TIME  
YIELDS VS TIME

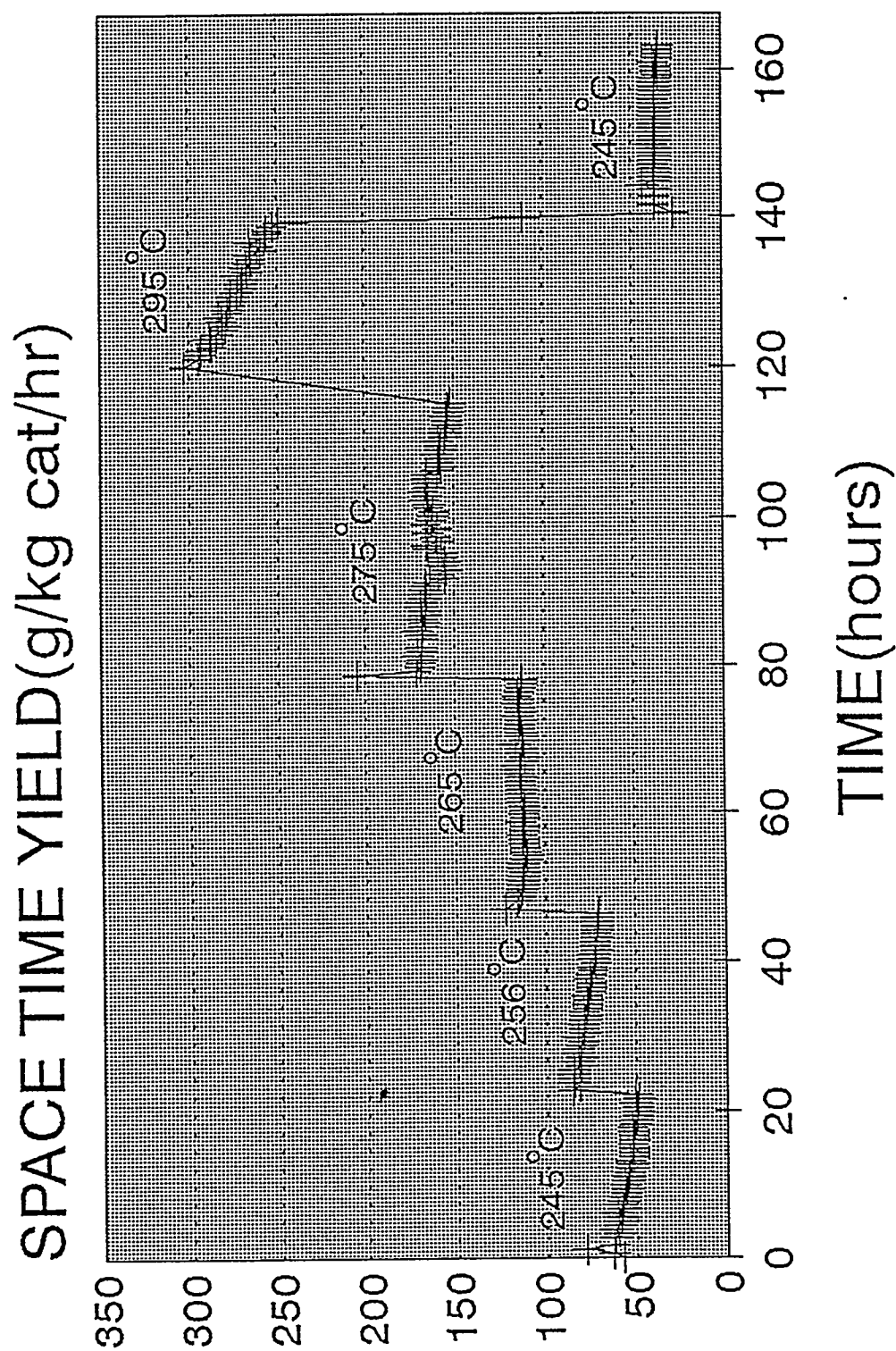


FIGURE 66. SELECTIVITY (C MOLE%)  
VS TEMPERATURE

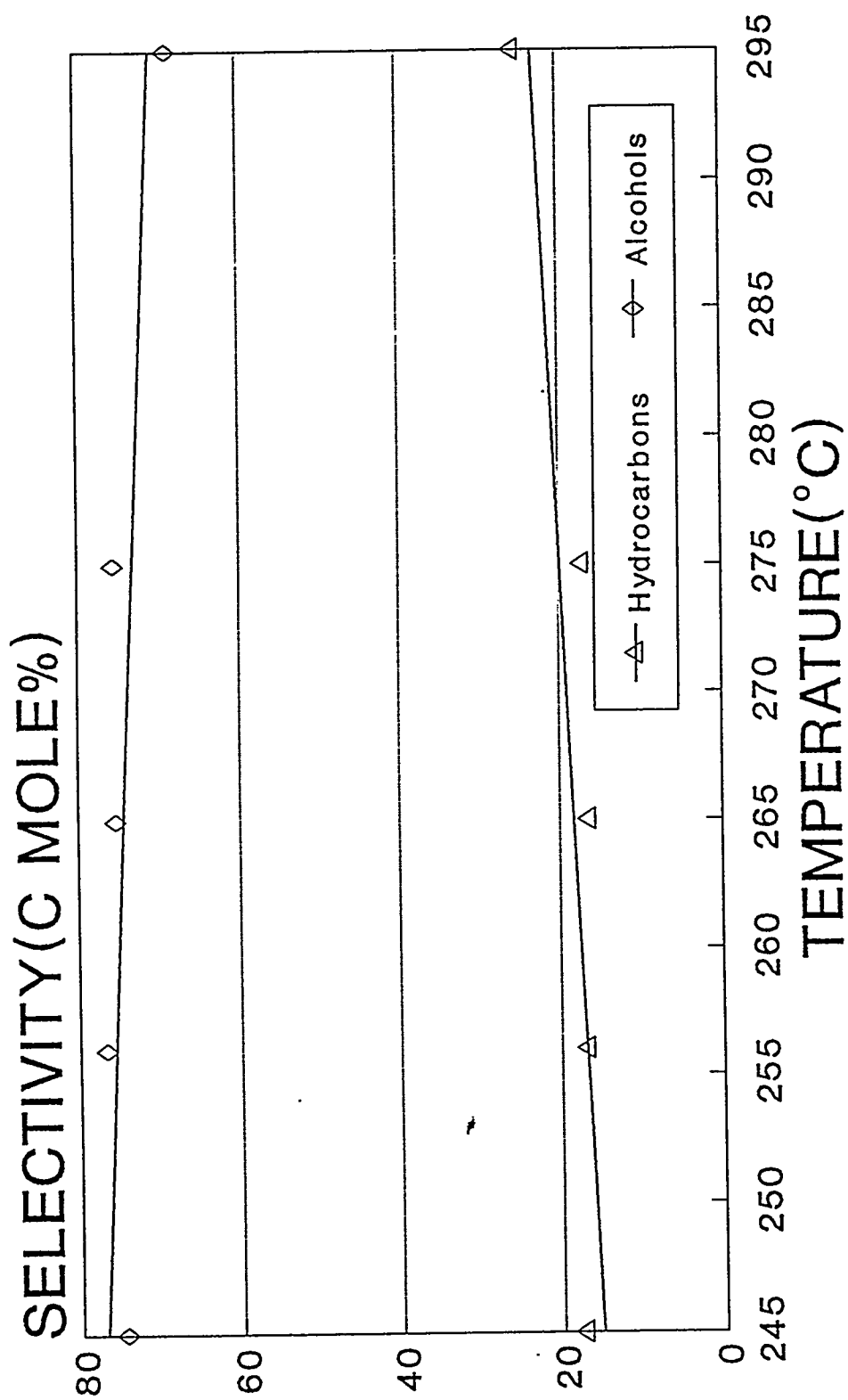


FIGURE 67. ALCOHOL/HYDROCARBON  
MOLAR RATIO VS TEMPERATURE

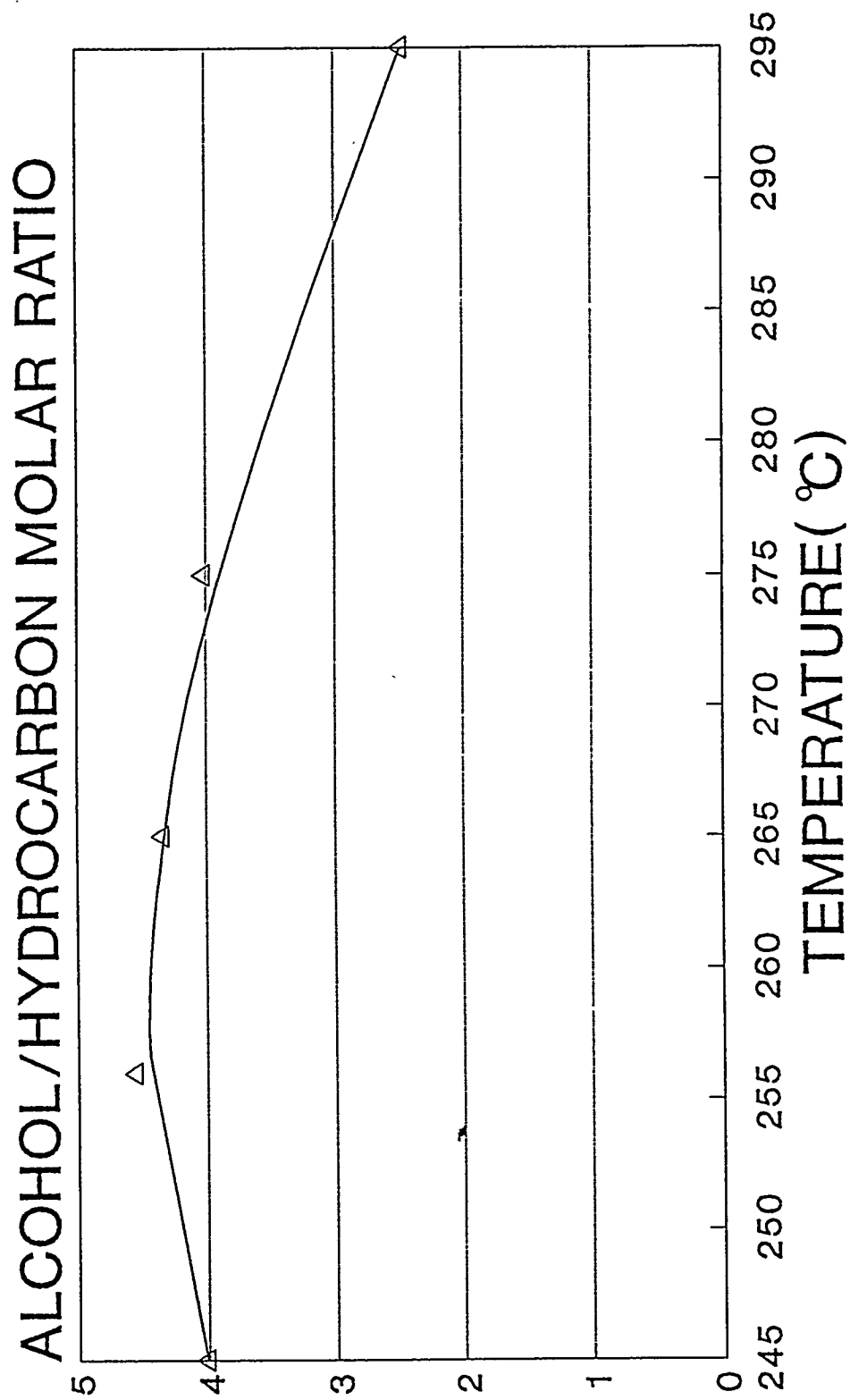
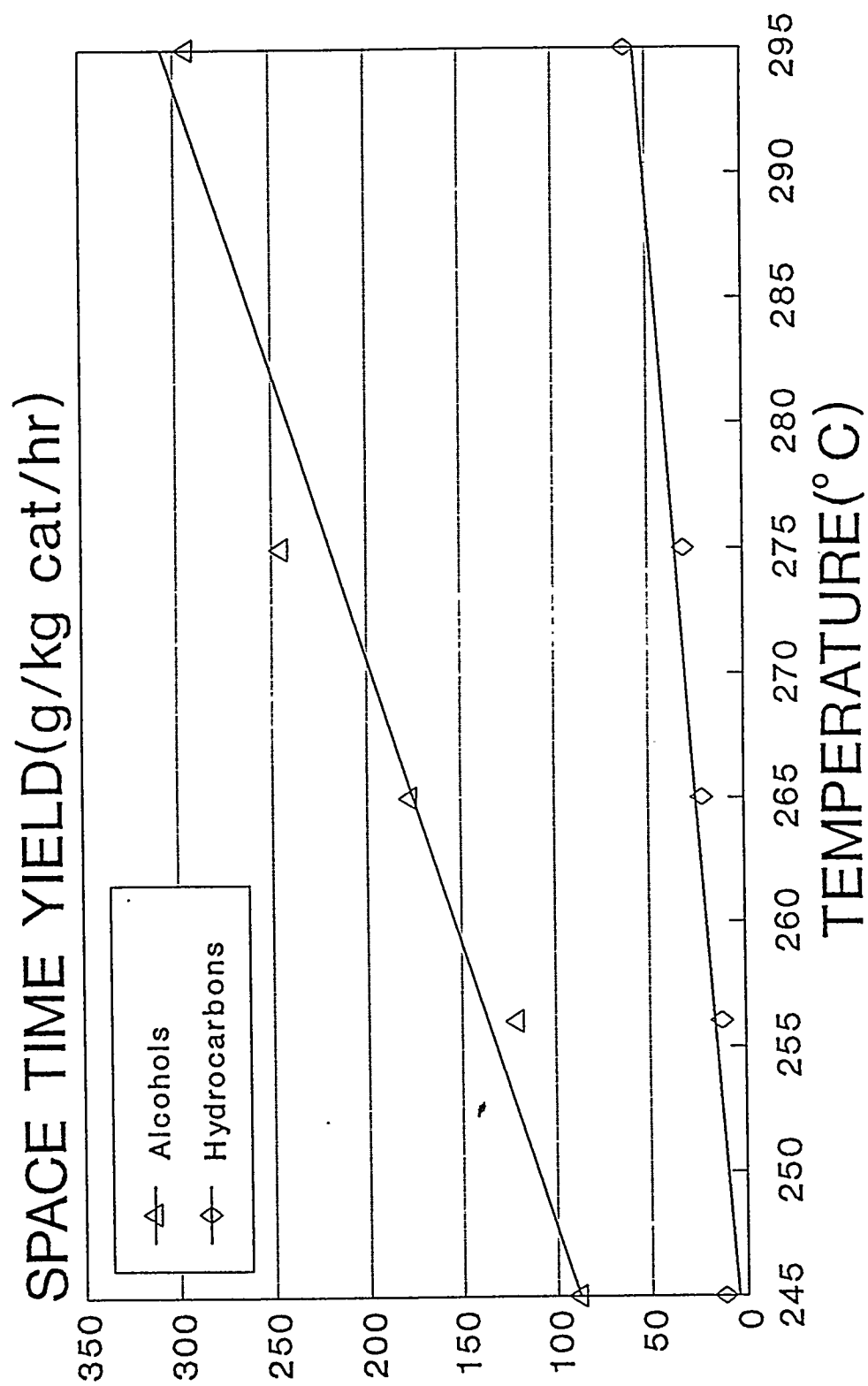




FIGURE 68. TOTAL ALCOHOL AND HYDROCARBON  
SPACE TIME YIELDS VS TEMPERATURE



# FIGURE 69. ALCOHOL SPACE TIME YIELDS VS TEMPERATURE

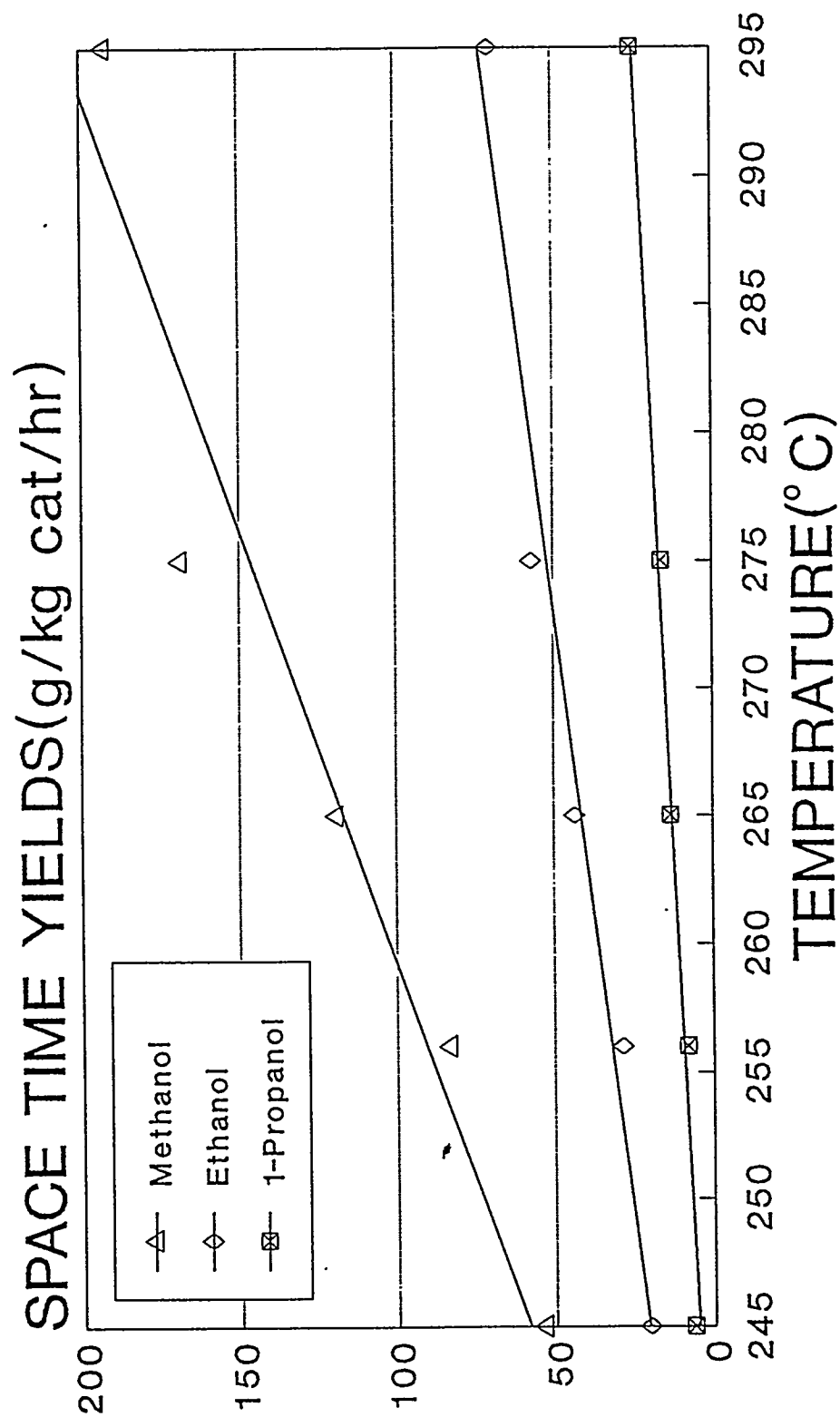
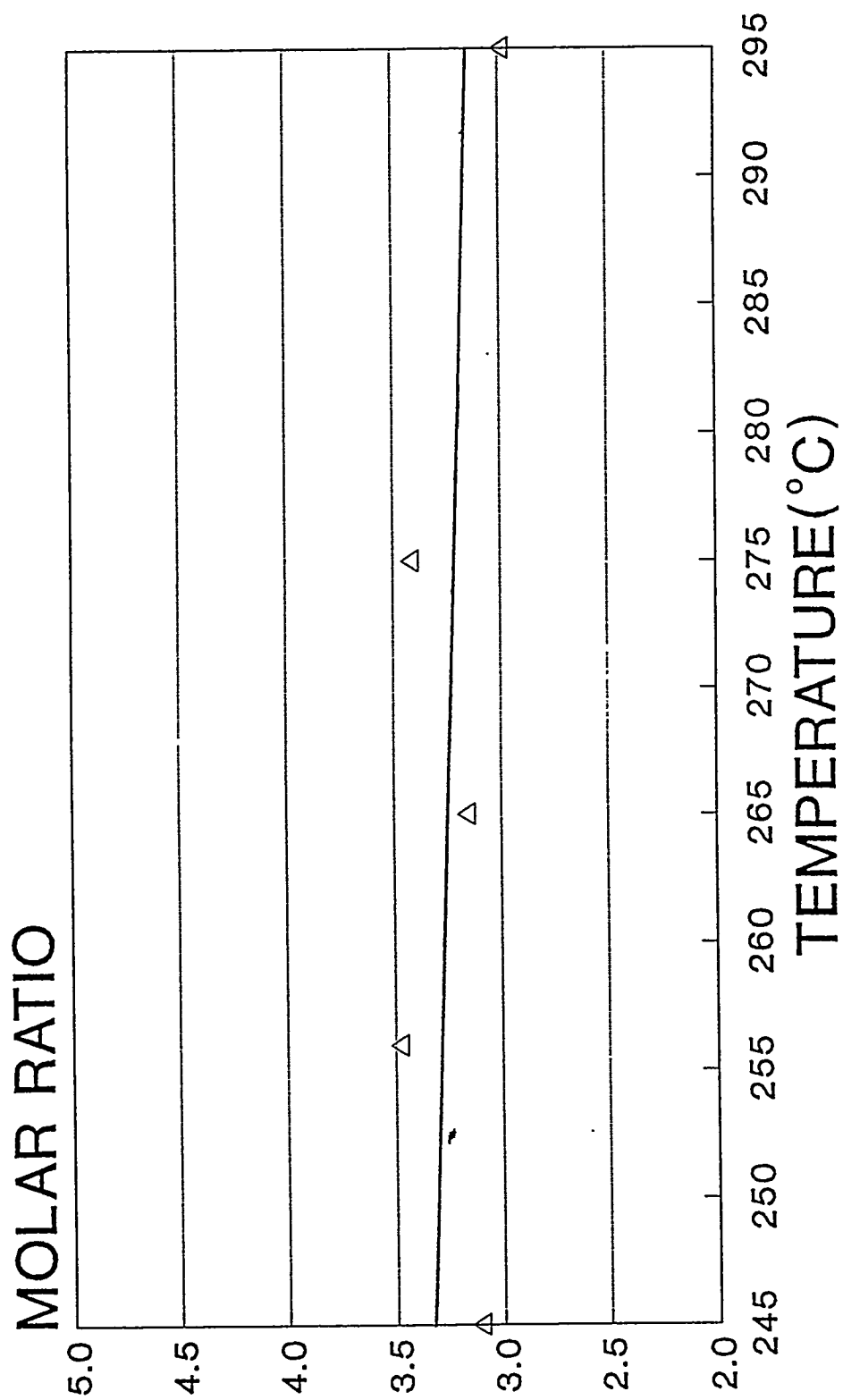


FIGURE 70. METHANOL/ $C_2^+$  ALCOHOL  
MOLAR RATIO VS TEMPERATURE



**TABLE 13.** Comparison of product space time yields (g/kg cat/hr) and CO conversion rates (mol CO/kg cat/hr) for (A) the present 10 wt% CsOOCH/MoS<sub>2</sub> catalyst with (B) those reported earlier [11,65] for a catalyst of the same composition under the same reaction conditions.

PRODUCT	245°C	256°C	265°C	275°C	295°C	Catalyst
Carbon Dioxide	55.48 52.47	75.48 79.74	113.69 136.83	159.06 166.66	273.71 317.10	A B
Water	-- tr	-- tr	-- tr	-- 0.49	1.59 3.66	A B
Methane	7.03 12.75	9.21 16.73	14.61 26.31	23.08 31.50	42.87 62.00	A B
Ethylene	0.79 0.28	0.96 0.76	1.06 0.68	0.98 0.63	1.07 0.92	A B
Ethane	2.55 0.92	2.80 2.01	4.35 4.18	5.87 5.71	11.72 13.52	A B
Propane	tr --	1.37 0.28	1.55 1.03	1.07 1.87	5.63 6.77	A B
Butane	-- --	-- --	-- --	tr --	tr 2.76	A B
Methanol	53.67 85.32	83.22 106.22	119.18 132.71	168.87 141.04	192.50 152.86	A B
Ethanol	20.16 24.12	28.55 32.96	43.47 48.87	56.83 52.75	70.06 62.70	A B
1-Propanol	6.17 5.06	7.78 7.54	13.11 12.71	15.74 14.93	25.04 22.23	A B
1-Butanol	-- --	-- tr	1.42 tr	3.62 tr	5.86 3.63	A B
Methyl Formate	tr 0.86	0.95 1.20	1.88 1.03	2.52 1.54	2.62 tr	A B
Methyl Acetate	5.20 1.30	5.09 1.96	7.97 2.63	9.06 2.88	9.23 1.33	A B
Acetaldehyde	2.19 --	2.54 --	3.83 --	4.90 --	5.77 --	A B
Propanal	-- --	-- --	2.34 --	3.05 --	3.93 --	A B
CO Conversion Rate (mol/kg cat/hr)	3.83 4.53	5.23 6.06	7.77 8.63	10.76 9.74	14.67 14.09	A B

temperature of 245°C, a lower productivity for methanol was noted (Figure 65), but the CO conversion level was hardly affected (Figure 62). In contrast, the total alcohol productivity was now higher (Figure 63), and this reflects the enhanced space time yields of the higher alcohols. At the same time, the productivity of the hydrocarbons was suppressed.

The surface area of the undoped MoS<sub>2</sub> catalyst was determined to be 90 m<sup>2</sup>/g. The doped CsOOCH/MoS<sub>2</sub> catalyst exhibited a surface of 36 m<sup>2</sup>/g, which was appreciably higher than the value usually observed for fresh Cs-doped MoS<sub>2</sub> catalysts, as will be discussed later in this report. Upon catalytic testing, a still lower surface area is usually obtained.

#### **X-Ray Powder Diffraction Analysis of MoS<sub>2</sub> Catalysts**

The conversion of the precipitated and dried MoS<sub>3</sub> to MoS<sub>2</sub> by calcination is a highly exothermic reaction. This step is carried out in an 8 mm ID quartz tube about 60 cm long that is heated by a horizontal tube furnace. Our most recent preparations employed sample sizes consisting of 2-3 g of MoS<sub>3</sub> that were mixed with 3 mm Pyrex beads. This mixture was then centered in the tube by using additional layers of Pyrex glass wool and additional Pyrex beads. During the calcination process, a constant flow of helium, nitrogen, or other gas was maintained (typically 60 ml/min). The thermal program consisted of increasing the temperature up to 200°C quickly using a differential heating devise and holding for 10 min. Then the temperature was increased to 450°C for 1.5 hr, after which the sample was cooled in the flowing gas. As pointed out in the Experimental section, the sulfur released by the decomposition of the MoS<sub>3</sub> to form MoS<sub>2</sub> was condensed on Pyrex beads at the cool outlet of the tube.

It became evident that temperature control during the exothermic decomposition

reaction was difficult when large sample sizes were used. Thus, X-ray powder diffraction (XRD) characterization of the samples was carried out to monitor the purity and crystallite size of the  $\text{MoS}_2$ . In addition, doping of the samples with cesium formate had been carried out, and XRD analysis of some of the Cs-doped samples was also carried out.

As described in the Experimental Section, two large batches of  $\text{MoS}_2$  were prepared from two batches of  $\text{MoS}_3$  that had been synthesized by coprecipitation from aqueous solution. The calcination of the  $\text{MoS}_3$  was carried out using 2-3 g samples and the products of several of these portions were combined to form the two larger batches of  $\text{MoS}_2$ . Figures 71 and 72 show the XRD patterns obtained for the two batches, which are designated as 2A (decomposition under He flow) and 1B (decomposition under  $\text{N}_2$  flow). It is apparent that the patterns are nearly identical. The diffraction peaks exhibit appreciable width, which is indicative of small crystallite size of the  $\text{MoS}_2$ .

A portion of the 1B batch of  $\text{MoS}_2$ , as described in the previous technical progress report, was added to a measured quantity of an aqueous cesium formate solution, which was then evaporated to dryness under flowing nitrogen while maintaining constant stirring. The XRD pattern of the freshly prepared Cs/ $\text{MoS}_2$  catalyst, containing  $\approx 10$  wt%  $\text{CsOOCH}$ , is shown in Figure 73. The only dominant features in this pattern are the same  $\text{MoS}_2$  diffraction lines as seen in Figures 71 and 72.

In contrast, a portion of the Cs/ $\text{MoS}_2$  sample prepared from the 2A batch of  $\text{MoS}_2$  was allowed to stand in air for over three weeks before XRD analysis was carried out. The resultant XRD pattern is shown in Figure 74. By the presence of the new sharp diffraction line observed in the XRD pattern, it is evident that crystalline cesium formate has formed on the surface of the catalyst. From the sharpness of the lines, the  $\text{CsOOCH}$  crystallites are larger than 100 nm in diameter. It is proposed that upon standing in an ambient

FIGURE 71

Sample: 2A File: MD6J02.SM

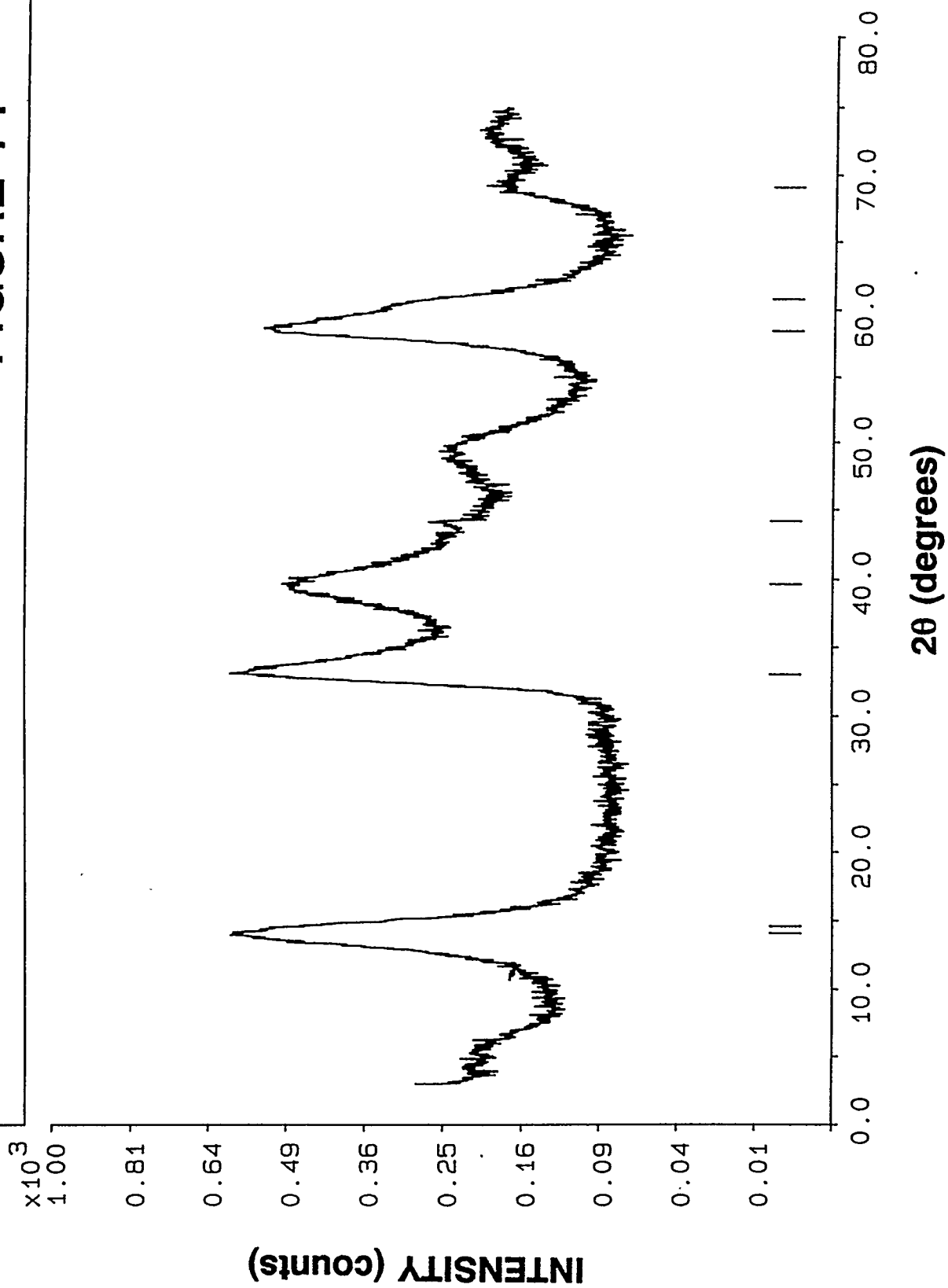


FIGURE 72

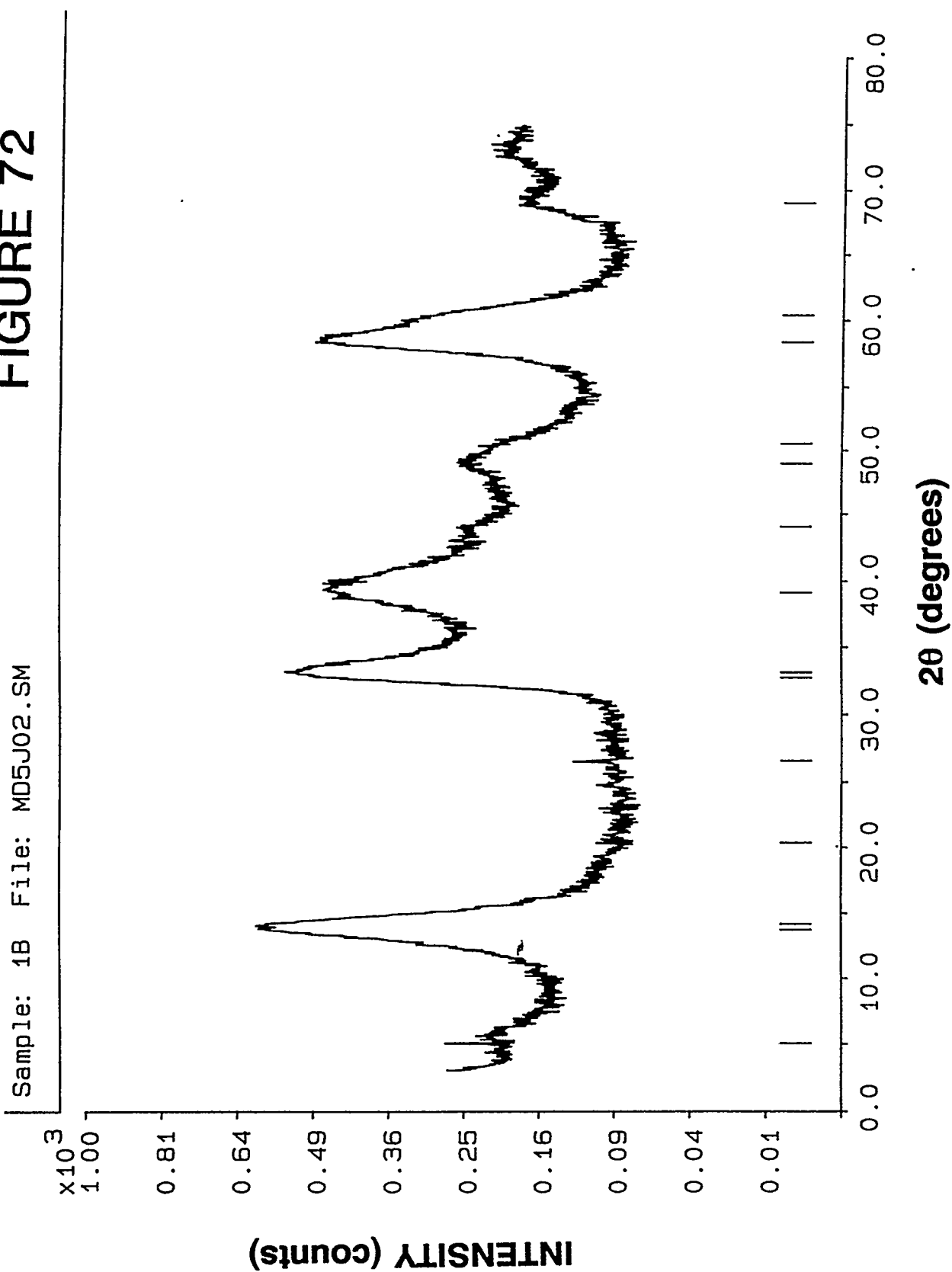




FIGURE 73

Sample: 2B File: MD7J02.SM

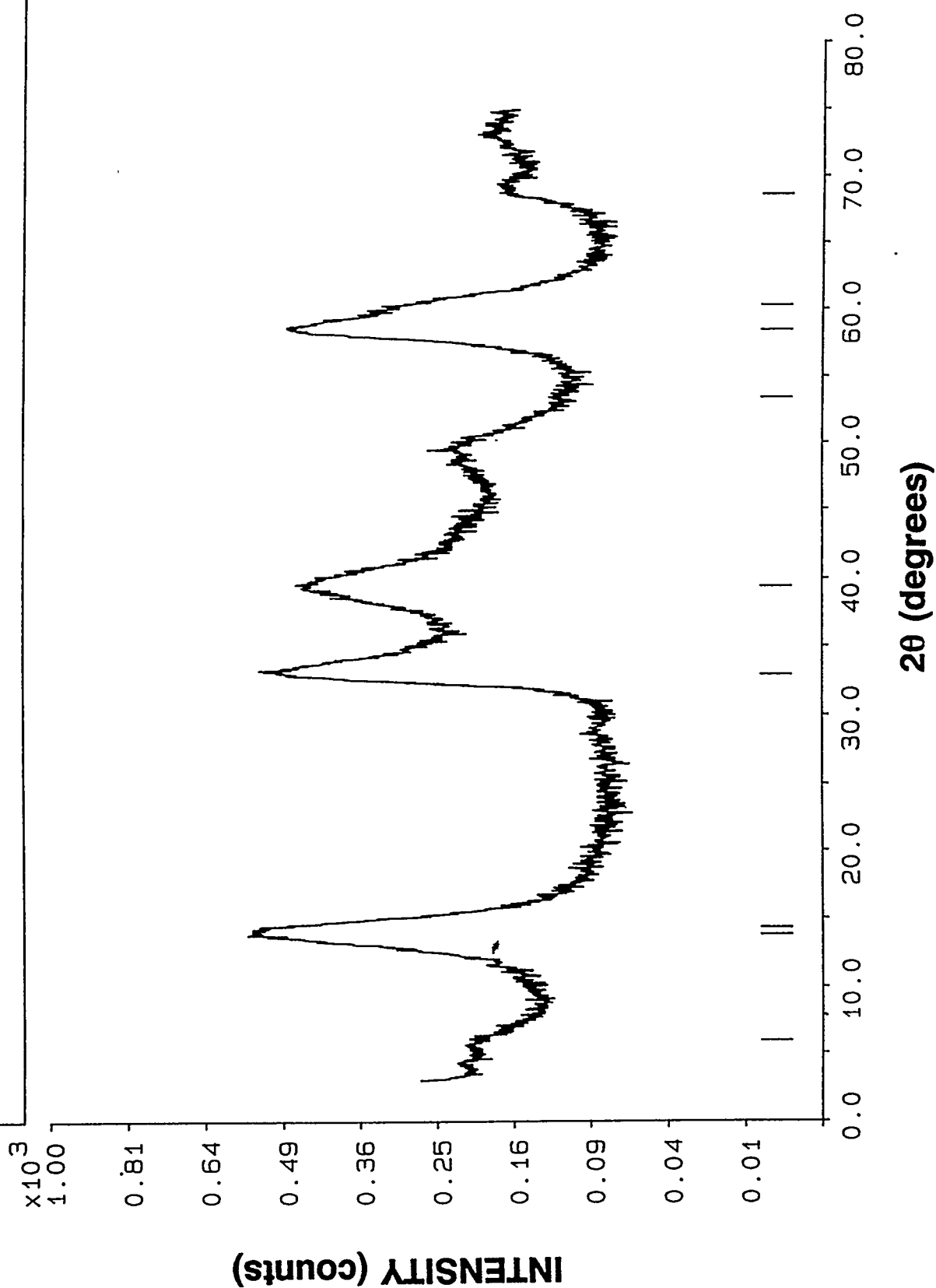
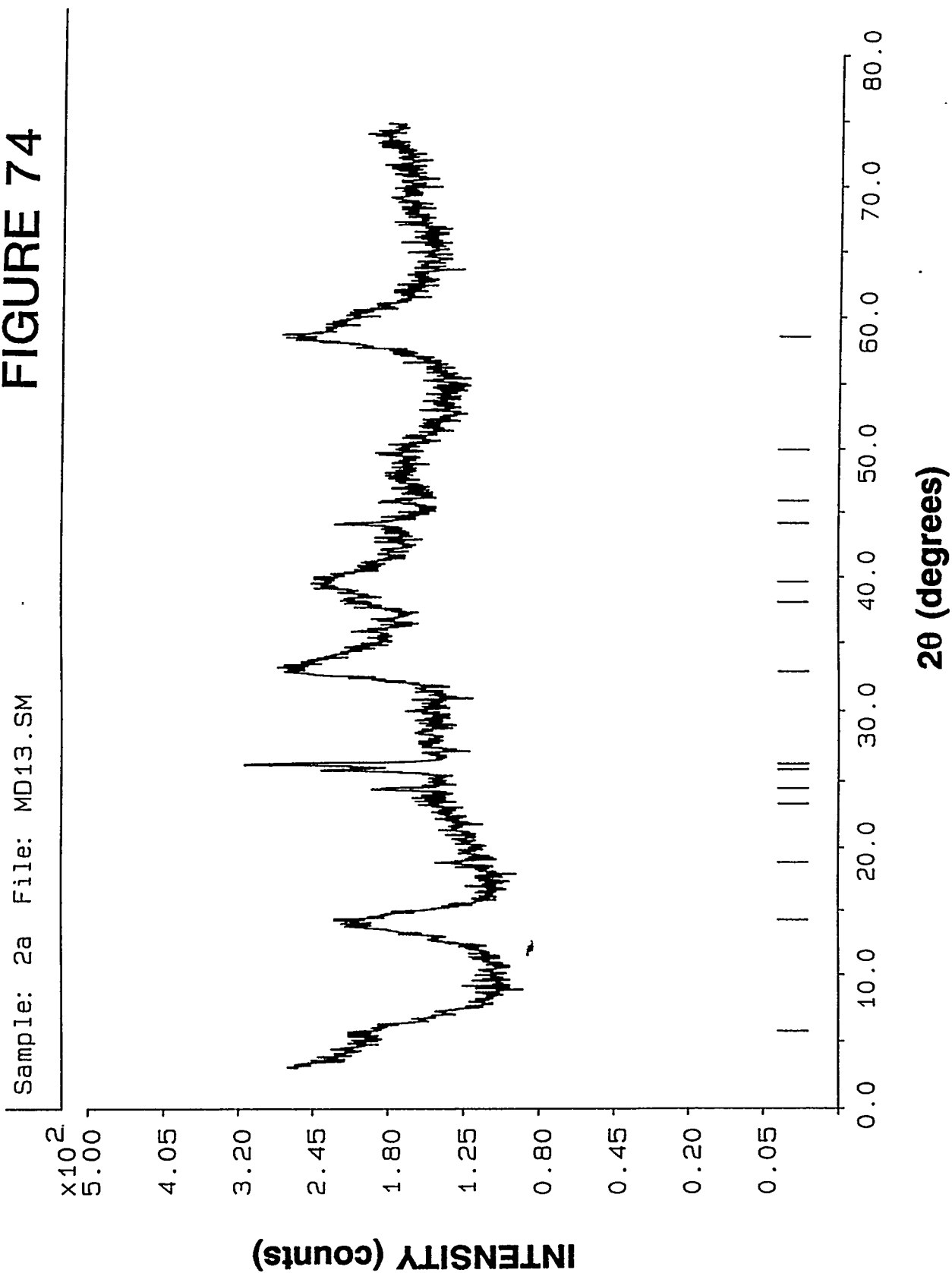


FIGURE 74



atmosphere, the Cs dopant that had initially been present in a dispersed state has migrated, agglomerated, and crystallized into large particles of cesium formate. Thus, upon use under catalytic conditions for alcohol synthesis from  $H_2/CO$  synthesis gas, the cesium dopant would likely exist as a segregated component that would not provide the high conversion of reactants to alcohols that is desirable.

An additional series of experiments was carried out with a third batch of  $MoS_2$ . After being prepared by calcination of  $MoS_3$ , doping of the  $MoS_2$  was carried out as for the samples described above to provide a doping level of  $\approx 10$  wt%  $CsOOCH$ . This sample was stored in a sealed vial, and the XRD pattern for the freshly prepared sample is shown in Figure 75. This sample was then allowed to stand in ambient atmosphere for a prolonged period of time ( $>1$  month), and the resultant XRD pattern is shown in Figure 76. Very sharp strong diffraction lines for cesium formate are evident in Figure 76.

Catalytic testing of an analogous air-exposed 10 wt%  $CsOOCH/MoS_2$  sample for alcohol synthesis from  $H_2/CO = 1$  synthesis gas at 8.2 MPa and  $295^\circ C$  was carried out in the continuous flow gas phase reactor system ( $GHSV = 7750$   $\ell/kg$  cat/hr) after reductive pretreatment at  $400^\circ C$  in flowing 2.04 vol%  $H_2/97.96$  vol%  $N_2$  (60 ml/min) for 1 hr. Alcohols (dominant product) and hydrocarbons were formed, as expected, but the overall catalytic activity was only about half of that expected for the Cs doping level utilized with this catalyst. The XRD pattern of the tested catalyst is shown in Figure 77, and the presence of a small quantity of cesium formate in this sample is evident. Therefore, the catalyst samples used for catalytic testing should be freshly prepared and not allowed to stand in ambient atmospheres, i.e. those containing oxygen, water vapor, and carbon dioxide.

FIGURE 75

Sample: 130 File: MD10J03.SM

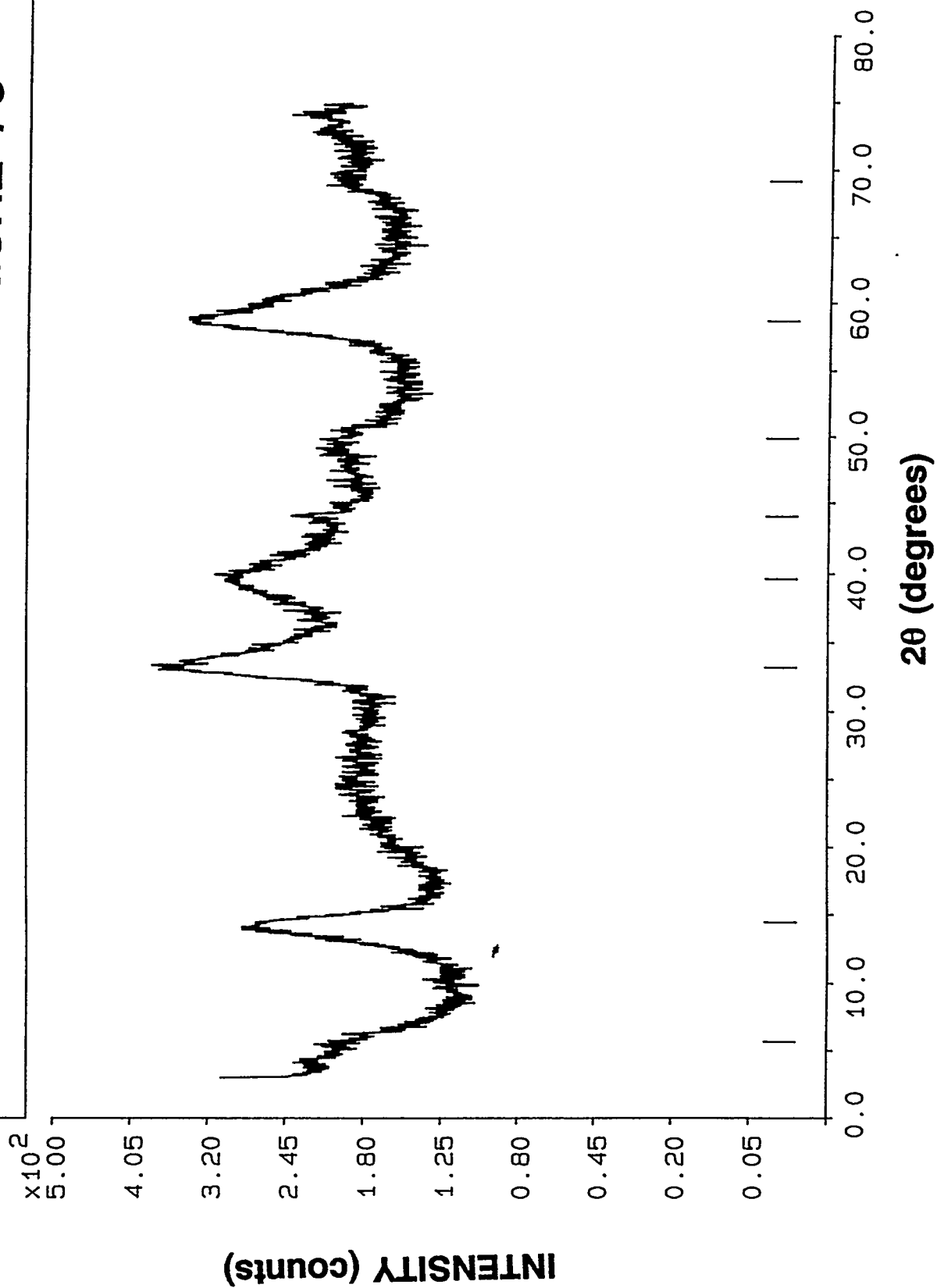


FIGURE 76

Sample: File: MD8J03.SM

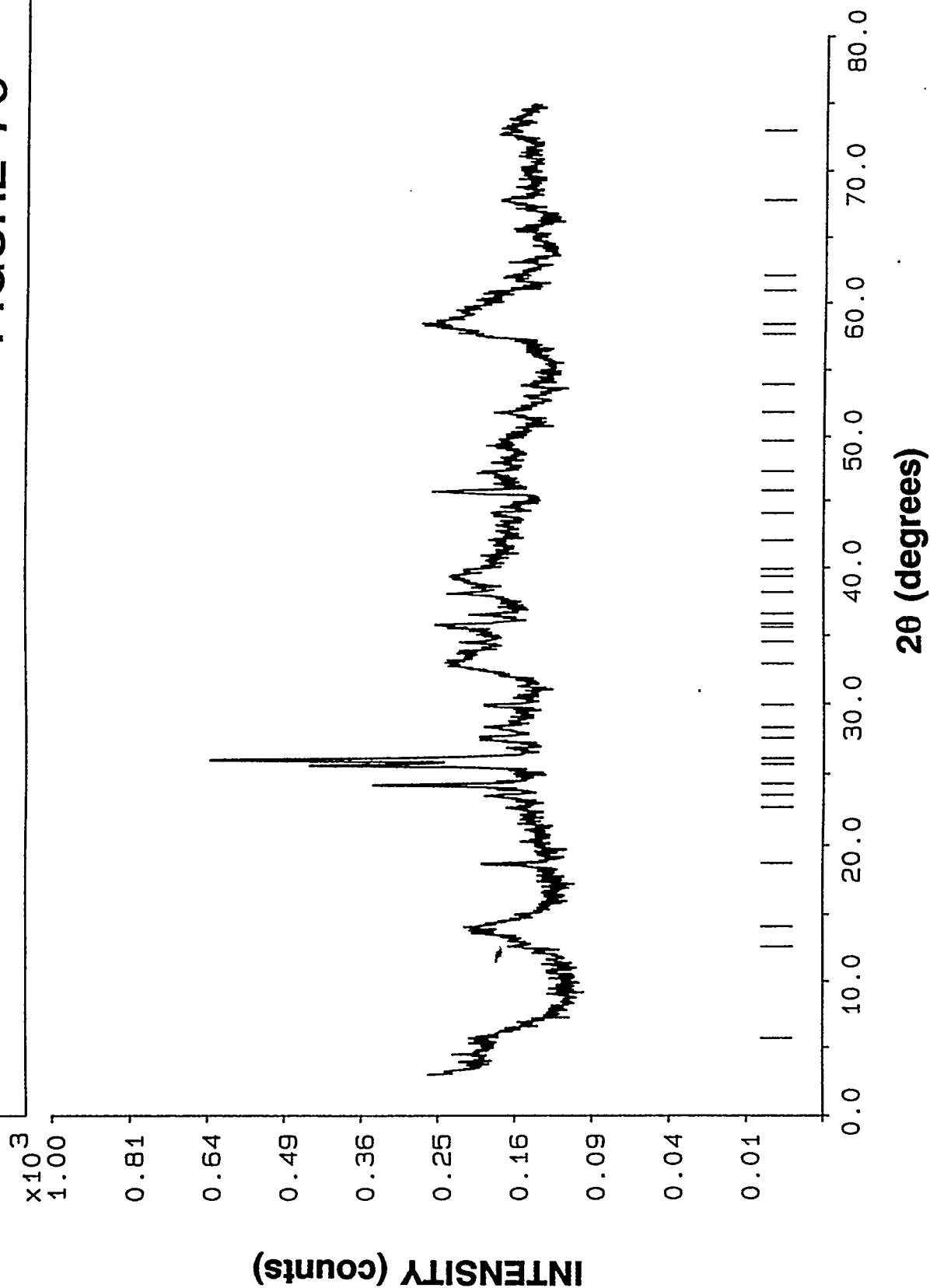


FIGURE 77

Sample: USED File: MD9J03.SM

